The Plant Cell, Vol. 12, 1127–1136, July 2000, www.plantcell.org © 2000 American Society of Plant Physiologists

Ca^{2+}-Stimulated Exocytosis in Maize Coleoptile Cells

Jens-Uwe Sutter, Ulrike Homann, and Gerhard Thiel[1]

Albrecht-von-Haller Institute for Plant Sciences, Plant Biophysics, Untere Karspüle 2, 37073 Göttingen, Germany

Changes in membrane capacitance (C_m) after photolysis of the caged Ca^{2+} compound dimethoxynitrophenamine were studied in protoplasts from maize coleoptiles. Changes in C_m values resulting from increased concentrations of free Ca^{2+} in the cytoplasm ($[Ca^{2+}]_{cyt}$) were interpreted as representing changes in $[Ca^{2+}]_{cyt}$–sensitive exocytosis and endocytosis. A continuous increase in $[Ca^{2+}]_{cyt}$ resulted in a sigmoidal increase in C_m values with a half-maximal concentration at ~1 μM. The steep increase in C_m values was followed by a variable slow phase in changing C_m values. When $[Ca^{2+}]_{cyt}$ increased at a rate of 0.6 μmol L^{-1} sec^{-1}, the initial steep increase in C_m values lasted ~5 to 10 sec. During this time, protoplasts increased in surface area by ~2.5%. The biphasic dynamics of $[Ca^{2+}]_{cyt}$–stimulated increases in C_m values can be described by a kinetic model containing two pools of vesicles with two $[Ca^{2+}]_{cyt}$–sensitive steps in the exocytotic pathway.

INTRODUCTION

For cell elongation, new membranes, proteins, and polysaccharide compounds must be delivered to the plasma membrane–cell wall interface (reviewed in Napier and Venis, 1995). Comparative electron microscopic studies of elongating cells in the apex of grass coleoptiles have shown that growing cells have increased numbers of dictyosomes and secretory vesicles in the cytoplasm (Quaite et al., 1983). This suggests that a growth-augmented demand for secretory activity is achieved by enhanced synthesis of vesicular membranes and transport cargo. An increase in secretory activity could therefore be viewed simply as the consequence of mass action driven by a greater number of secretory vesicles.

In recent electrophysiological studies, the secretory activity of maize coleoptile protoplasts has been assayed by monitoring membrane capacitance (C_m) (Thiel et al., 1994). This electrical variable is proportional to the surface area of the membrane and allows in vivo monitoring of changes in area related to exocytosis and endocytosis (Neher and Marty, 1982; Homann and Tester, 1998). The perfusion of protoplasts from maize coleoptiles containing a high concentration of cytoplasmic free Ca^{2+} ($[Ca^{2+}]_{cyt}$) (1 μM) caused a continuous increase in membrane capacitance. In contrast, membrane capacitance did not increase when protoplasts were perfused with low $[Ca^{2+}]_{cyt}$ (Thiel et al., 1994). This result suggests that high concentrations of $[Ca^{2+}]_{cyt}$ stimulate processes in the secretory pathway of these as well as many other eukaryotic cells (reviewed in Kasai, 1999), including plant cells (Zorec and Tester, 1992; Homann and Tester, 1997; Carroll et al., 1998). In experiments with coleoptile protoplasts, C_m values started to increase within seconds after the increase in $[Ca^{2+}]_{cyt}$ (Thiel et al., 1994, 2000). Because the synthesis of secretory vesicles occurs in a time frame of minutes (e.g., Phillips et al., 1988), however, not seconds, the rapid response of membrane capacitance to $[Ca^{2+}]_{cyt}$ excludes the possibility that the increase in secretory activity depends only on a $[Ca^{2+}]_{cyt}$–stimulated synthesis of secretory vesicles. Hence, $[Ca^{2+}]_{cyt}$ must influence the secretory pathway downstream of where the secretory vesicles are produced.

In this study, the effect of $[Ca^{2+}]_{cyt}$ stimulation on the secretory pathway was further examined by making use of the rapid increase of $[Ca^{2+}]_{cyt}$ when Ca^{2+} is released from the caged Ca^{2+} compound 1-(2-nitro-4,5-dimethoxyphenyl)-1,2-diaminoethane-*N*,*N*,*N*′*N*′-tetraacetic acid (dimethoxynitrophenamine, or DMN) and simultaneously recording the membrane capacitance. We found that the rapid increase of $[Ca^{2+}]_{cyt}$ resulted in a rapid increase in membrane capacitance followed by a more variable second phase. The latter consisted of either a continuous but slower increase in C_m values or a decrease. We conclude that the late stage of the secretory pathway is dominated by two serially arranged pools of vesicles in these cells. Ca^{2+} augments both forward steps from an upstream pool into exocytosis.

RESULTS

Increase of $[Ca^{2+}]_{cyt}$ Causes an Increase in Membrane Capacitance

To examine whether changes in surface area were dependent on the concentration of $[Ca^{2+}]_{cyt}$, we measured $[Ca^{2+}]_{cyt}$

[1] To whom correspondence should be addressed. E-mail gthiel@gwdvms.dnet.gwdg.de; fax 49-551-397838.

and membrane capacitance simultaneously. C_m values were taken to be proportional to the plasma membrane surface area (Neher and Marty, 1982; Thiel et al., 1994; Homann and Tester, 1998). Figure 1 shows measurements of membrane capacitance in a protoplast from the apex of a maize coleoptile. After achieving the whole-cell configuration, the cell was perfused with standard buffer solution (see Methods) from the patch pipette. The Ca^{2+} concentration of this perfusion buffer was ~4 nM (Xu et al., 1997). Perfusing the cytoplasm with this low-Ca^{2+} solution generally caused a slight decrease in C_m values during the first few minutes, after which the C_m values stabilized. Frequently, we found that the membrane conductance (G_m) also decreased slowly over a period of minutes. A representative tracing of G_m values is shown in Figure 1.

After allowing sufficient time for equilibrating the cytoplasm with the pipette solution (see Methods), $[Ca^{2+}]_{cyt}$ was increased continuously from the low, resting value to micromolar concentrations. Figure 2 shows an enlargement of the electrical cell settings and the $[Ca^{2+}]_{cyt}$ recording from Figure 1 before and during the increase of $[Ca^{2+}]_{cyt}$. Illumination of the protoplasts with UV radiation at 380 nm (UV_{380}) caused the release of Ca^{2+} from its caged precursor DMN, resulting in a roughly exponential relaxation in fluorescent light emission (F_{380}). This decrease in F_{380} values can be converted into $[Ca^{2+}]_{cyt}$ by using Equation 1 (see Methods). In this case, $[Ca^{2+}]_{cyt}$ increased over the 13.1 sec of illumination from 4 nM to ~6 μM. Stimulated by this ramp elevation of $[Ca^{2+}]_{cyt}$, C_m values increased sigmoidally (Figure 2).

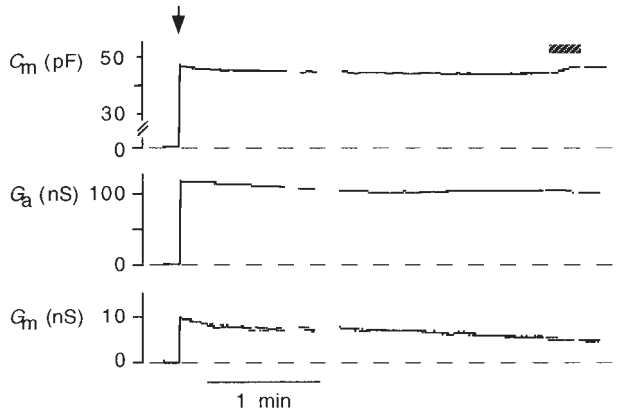

Figure 1. Time Course of Membrane Capacitance, Access Conductance, and Membrane Conductance of a Coleoptile Protoplast during Perfusion of the Cytoplasm with a Pipette Solution Containing Low $[Ca^{2+}]_{cyt}$.

The arrow marks the time of breaking into whole-cell configuration. During the time indicated by the shaded bar, the protoplast was illuminated by UV_{380} to release Ca^{2+} from the caged precursor. Dashed lines indicate zero values for electrical variables. G_a, access conductance. pF, picofarad; nS, nanosimens, i.e., gigaohm^{-1}.

In the example shown in Figure 2, membrane conductance remained unaffected during the increase in membrane capacitance. This observation was confirmed by other measurements. Figure 3 shows a plot of $[Ca^{2+}]_{cyt}$–stimulated increases in C_m values versus the corresponding changes in G_m values from 13 randomly chosen experiments. The plot confirms that increases in membrane capacitance and hence in surface area were not correlated with a concomitant increase in membrane conductance. This means that the extra membrane incorporated during the increase of cytosolic free Ca^{2+} did not insert an appreciable amount of additional active transporters, such as channels or pumps, into the plasma membrane.

To test whether the $[Ca^{2+}]_{cyt}$–stimulated increase in membrane capacitance (CARC) depended specifically on the increase of $[Ca^{2+}]_{cyt}$, DMN was loaded with Mg^{2+}. All Ca^{2+} in the pipette solution was therefore replaced by Mg^{2+}. By the same procedure as was used for collecting the data shown in Figure 2, membrane capacitance was monitored after illuminating the protoplast with UV_{380} to liberate Mg^{2+} from the cage. In this case, F_{380} (i.e., the marker for $[Ca^{2+}]_{cyt}$) remained unaffected, as was expected. Also, membrane capacitance was not affected by illumination (Figure 4). This result, which was confirmed in three other experiments, shows that the increase in C_m values in illuminated samples is specifically related to the increase of $[Ca^{2+}]_{cyt}$; it cannot be mimicked by Mg^{2+}. Furthermore, the finding demonstrates that neither UV_{380} light nor the byproduct of photolysis affects membrane capacitance.

Kinetics of CARC

A $[Ca^{2+}]_{cyt}$–stimulated increase in C_m values was observed in 11 of 15 protoplasts in which $[Ca^{2+}]_{cyt}$ was increased by 0.6 ± 0.25 μmol L^{-1} sec^{-1}. Figure 5A illustrates the scope of normalized CARC in these 11 protoplasts during ramp increases in $[Ca^{2+}]_{cyt}$. The plot shows that at the start of photolysis, C_m values rose sigmoidally, showing a steep increase over approximately the first 5 to 7 sec. After this initial phase of rapid increase, changes in C_m values in different protoplasts varied greatly. C_m values continued to increase, albeit more slowly than initially. In other cases, C_m values returned to those at the resting level. This decrease in membrane capacitance means that the membrane added to the plasma membrane during enhanced exocytosis is in some cases reclaimed by endocytosis. The variability of the second phase in CARC under conditions of increased $[Ca^{2+}]_{cyt}$ was not a characteristic of different types of protoplasts. Figure 5B shows that the difference in late responses could be observed even within one protoplast treated with repeated increases of $[Ca^{2+}]_{cyt}$.

The speed of $[Ca^{2+}]_{cyt}$–stimulated ΔC_m correlated with the speed of the increase in $[Ca^{2+}]_{cyt}$. Figure 6A shows three examples of CARCs with different velocities during an increase in $[Ca^{2+}]_{cyt}$. The rise in C_m values increased with increasing

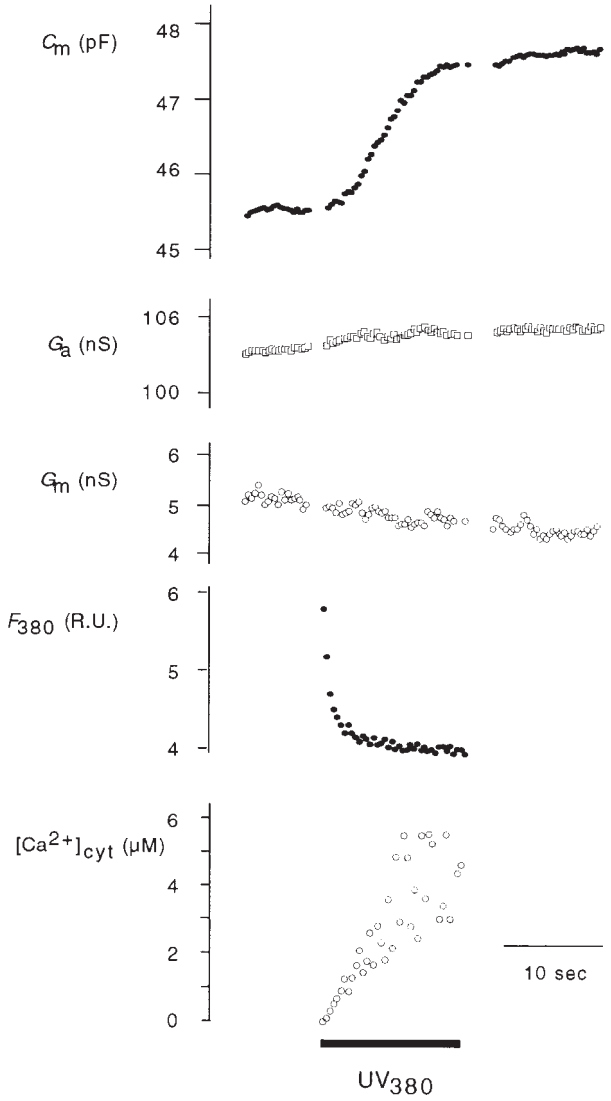

Figure 2. Ramp Elevation of $[Ca^{2+}]_{cyt}$ Stimulates an Increase in CARC in Maize Coleoptile Protoplast.

Enlargement of cell parameters from the section in Figure 1 indicated by the bar before and during illumination with UV light. The relaxation of fluorescence at 380 nm (F_{380}) was used to calculate $[Ca^{2+}]_{cyt}$ with Equation 1. The solid bar indicates the time of illumination with UV light. G_a, access conductance; R.U., relative units.

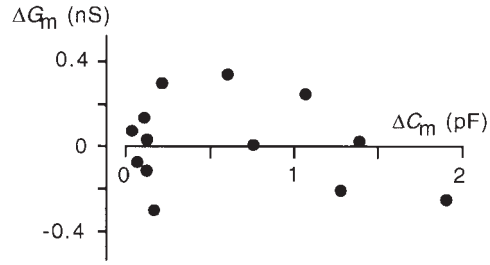

Figure 3. CARC Does Not Cause a Measurable Increase in Membrane Conductance.

ΔG_m and ΔC_m values were measured isochronally after the increase of $[Ca^{2+}]_{cyt}$ as a deviation of membrane conductance and membrane capacitance from the resting value at low values for $[Ca^{2+}]_{cyt}$ (n =13 protoplasts).

rates of $[Ca^{2+}]_{cyt}$ elevation. Figure 6B illustrates the maximal rate for the increase in membrane capacitance during the linear phase of $[Ca^{2+}]_{cyt}$ increase. As the plot shows, the stimulating effect of $[Ca^{2+}]_{cyt}$ on C_m values saturates at a rate >3 μmol L^{-1} sec^{-1}. Fitting a Michaelis-Menten–type kinetic to the data yielded a maximal membrane capacitance increase rate of 2.9% sec^{-1} over the resting capacitance ($C_{m,0}$). The half-maximal rate of CARC was achieved when $[Ca^{2+}]_{cyt}$ increased at a rate of 0.49 μmol L^{-1} sec^{-1}.

To quantify the relationship between changes in C_m values and $[Ca^{2+}]_{cyt}$, we plotted ΔC_m versus the corresponding $[Ca^{2+}]_{cyt}$ values. Figures 7A to 7C show the typical sigmoidal relationship between the two variables. In this example, we estimated a Ca^{2+} concentration for half-maximal stimulation at 0.92 μM (mean ±SD, 0.93 ± 0.17 μM; n = 5 protoplasts) and a slope of 0.27% μM^{-1} $[Ca^{2+}]_{cyt}$ for the increase between 10 and 90% of C_m (mean ±SD, 1.13 ± 0.4% μM^{-1} $[Ca^{2+}]_{cyt}$, n = 5 protoplasts).

Amplitudes of CARCs

To estimate the maximal area gain in CARCs, we plotted the amplitudes of individual CARCs versus $C_{m,0}$ values of the respective protoplasts. For this purpose, only CARCs with a clear saturation were considered (e.g., Figure 8, top). In addition, only data from the first $[Ca^{2+}]_{cyt}$ stimulation for one protoplast were taken into account. The plot shown in Figure 8 (bottom) reveals only a weak correlation between amplitude of CARCs and resting capacitance. A regression line through the origin and data in Figure 8 has a slope of 2.4% and a regression coefficient of 0.87.

Amplitude of CARC Increases with Time after a Preceding Increase in C_m Values

One feature of CARC was that C_m values leveled off or even decreased when $[Ca^{2+}]_{cyt}$ was still increased (Figure 5). In keeping with results from studies with animal cells (Heinemann et al., 1993, 1994), this biphasic increase in C_m

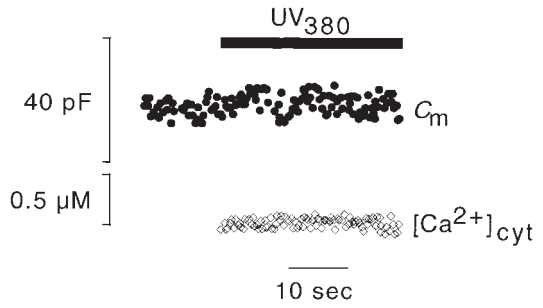

Figure 4. Mg^{2+} Does Not Trigger an Increase in Membrane Capacitance.

Membrane capacitance and $[Ca^{2+}]_{cyt}$ in protoplasts dialyzed with Mg^{2+}-loaded DMN were measured. Protoplasts were illuminated with UV_{380} to release Mg^{2+} from the cage. The bar indicates time of illumination.

values suggests that a rapid form of exocytosis is limited by a depletable pool of vesicles. To test this possibility, we increased the $[Ca^{2+}]_{cyt}$ value repeatedly within the same protoplast. Figure 9A shows the results of an experiment in which C_m values had increased in a typically sigmoidal manner when $[Ca^{2+}]_{cyt}$ was increased. After 155 sec, $[Ca^{2+}]_{cyt}$ was increased a second time. This second increase in $[Ca^{2+}]_{cyt}$ also resulted in a small increase in C_m values. A comparison of the first and second CARC values obtained under this condition shows that the kinetics are similar, but the amplitude of the second one is much smaller (Figure 9A). In similar experiments, we found that the amplitude of the second response increased in relation to that of the first one and as a function of the interval between stimulations. Figure 9B shows a plot of the ratios of amplitudes of the second CARC over the first as a function of the time between Ca^{2+} stimulations. Assuming that the dependency of a second CARC on the intervening time between stimulations reflects a refilling of a depletable pool, then a minimum of ~200 sec after depletion must pass before the pool reaches 50% of its initial content.

Frequently, the $[Ca^{2+}]_{cyt}$–stimulated increase in membrane capacitance was followed by a decrease in membrane capacitance, that is, a phase of net endocytosis (Figure 5). In this context, we tested the possibility that vesicles reclaimed during this phase of endocytosis could be immediately recycled for exocytosis. Figure 10 shows a representative experiment in which the initial increase in $[Ca^{2+}]_{cyt}$ resulted in an increase in membrane capacitance, which was followed by a substantial phase of net endocytosis. Also, in this case, a second increase in $[Ca^{2+}]_{cyt}$ (129 sec after the first one) caused only a diminished increase in membrane capacitance. This shows that the membrane reclaimed during endocytosis is not directly available for exocytosis.

A Model for $[Ca^{2+}]_{cyt}$–Stimulated Exocytosis

A model describing the properties of $[Ca^{2+}]_{cyt}$–stimulated increases in C_m values must account for the following experimental observations: (1) a sigmoidal increase in membrane capacitance during ramp elevation of $[Ca^{2+}]_{cyt}$; (2) transient insensitivity of membrane capacitance to $[Ca^{2+}]_{cyt}$; and (3) the possibility of a decrease in membrane capacitance after CARC.

To describe these phenomena, we adopted a model used to explain similar $[Ca^{2+}]_{cyt}$–stimulated increases in membrane capacitance in chromaffin cells (Heinemann et al., 1993). In this model, two pools of vesicles, designated A and B, are connected in series, leading finally to exocytosis (pool C) (Figure 11A). Vesicles travel between pools A, B, and C with the forward rate constants k_a and k_c and a backward rate constant k_b. The occasional decrease in C_m values after a preceding increase underlines the fact that endocytosis into another pool, D, with a rate constant k_d, must also be

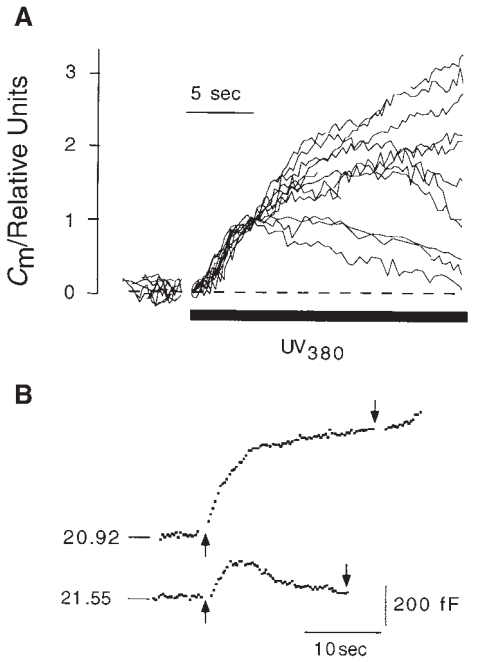

Figure 5. Protoplast-to-Protoplast Variability in Changes in C_m Values Stimulated by Ramp Elevation of $[Ca^{2+}]_{cyt}$.

(A) Membrane capacitance responses were determined from 11 protoplasts when $[Ca^{2+}]_{cyt}$ was increased in a ramplike fashion from 4 nM at a mean rate of 0.6 ± 0.25 μmol L^{-1} sec^{-1}.

(B) Two membrance capacitance responses stimulated by ramp elevation of $[Ca^{2+}]_{cyt}$ in the same protoplast. The time gap between stimulations was 169 sec. The time of illumination with UV light is marked by arrows. Numbers on membrane capacitance traces denote resting values in picofarads. Scale bars denote time in seconds and C_m values in femtofarads.

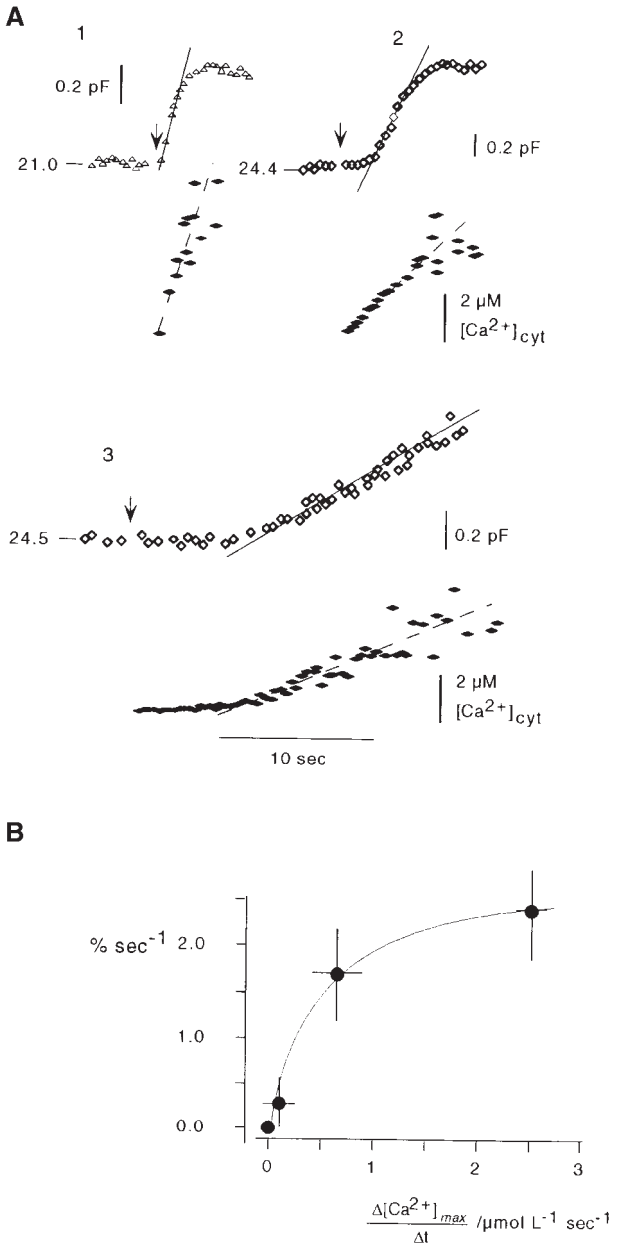

Figure 6. The Velocity of CARC Is a Function of the Rate of Increase in $[Ca^{2+}]_{cyt}$.

(A) Three representative examples (1, 2, and 3) show CARCs (open symbols) when $[Ca^{2+}]_{cyt}$ (solid symbols) is increased at different rates. Note that for low-intensity UV_{380} (trace 3), the increase in $[Ca^{2+}]_{cyt}$ is delayed. This effect probably reflects rebinding of uncaged Ca^{2+} to unphotolyzed DMN. Numbers on membrane capacitance traces denote resting values in picofarads.

(B) Plot of the rate in the increase of membrane capacitance (asymptotes in **[A]**) versus the rate of $[Ca^{2+}]_{cyt}$ increase during the linear phase. Data fitted (line) by using Michaelis-Menten kinetics yielded a maximal rate for CARC of 2.9% sec^{-1} over the resting capacitance with a half-maximal rate $\Delta Ca_{max}/\Delta t = 0.49$ μmol L^{-1} sec^{-1}.

considered. The best assumption is that the retrieved vesicles are not immediately fed back into pool B, because this pool could be completely depleted despite ongoing endocytosis. There was no indication that measurable endocytosis speeded the refilling of pool B (Figure 10). The often-observed increase in C_m values involving an initial fast phase followed by a slower second phase (e.g., Figure 5) further indicated that k_c must be larger than k_a.

The values for the rate constants were calculated on the basis of the equations given by Heinemann et al. (1993) in jointly fitted algorithms (see Methods). During this procedure, several data sets, derived from different protoplasts, were fitted together with one common set of rate constants

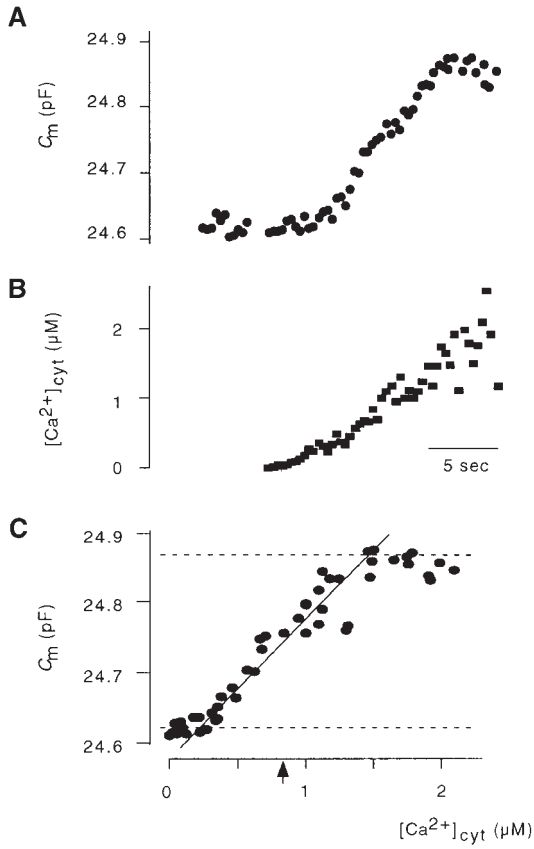

Figure 7. $[Ca^{2+}]_{cyt}$–Dependent Increase in Membrane Capacitance.

(A) and **(B)** Combined measurement of membrane capacitance and $[Ca^{2+}]_{cyt}$.

(C) Plot of Ca^{2+} versus C_m values. Dashed lines indicate asymptotes to $C_{m,0}$ (top) and the maximal amplitude of CARC (bottom). Asymptotes were drawn through the mean values of the first five and the highest five data points, respectively. The diagonal line illustrates the slope of the increase in C_m values. The slope between 10 and 90% of the increase in membrane capacitance (ΔC_m) is 0.27% (μmol $L^{-1})^{-1}$. The arrowhead denotes $[Ca^{2+}]_{cyt}$ for the half-maximal stimulation (0.92 μM).

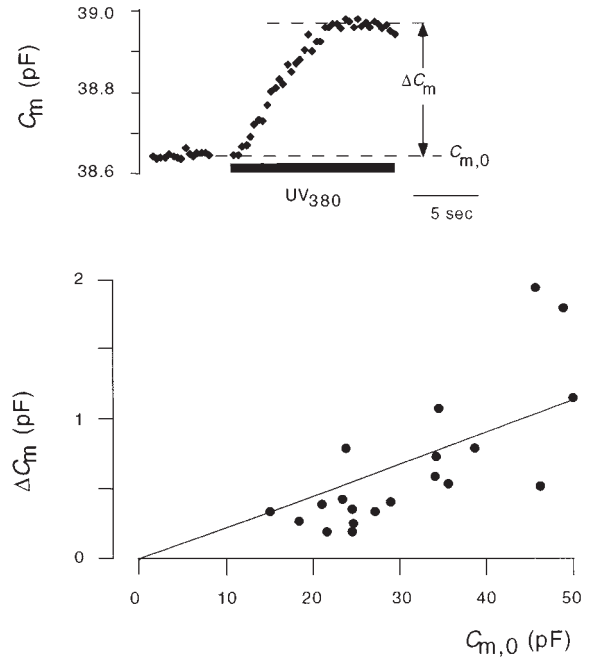

Figure 8. Amplitude of CARC as a Function of the Resting Capacitance before Stimulation.

In experiments in which ramp elevation of Ca^{2+} caused an increase in C_m values with a clear saturation (see inset, top), the amplitude, ΔC_m, was measured and plotted versus the $C_{m,0}$ value that was measured before Ca^{2+} stimulation. Linear fit (line) of data through the origin has a slope of 2.4%.

but with various pool sizes for each protoplast. The rationale for this approach was the assumption that the mechanisms underlying the secretory system are the same in cells from the same tissue, whereas the pool sizes may vary from cell to cell (Quaite et al., 1983). The pool sizes were estimated from the fitted amplitudes of increases in C_m values divided by the mean capacitance of secretory vesicles from this tissue (0.2 fF; Thiel et al., 1998) to obtain the number of vesicles residing in any one pool.

Various mathematical dependencies of the rate constants k_x for $[Ca^{2+}]_{cyt}$ were tested to obtain successful fits. The best results were achieved with the model shown in Figure 11A. According to this model, the forward steps k_a and k_c are accelerated by $[Ca^{2+}]_{cyt}$ in a linear manner because $k_a = a_a \cdot [Ca^{2+}]_{cyt}$ and $k_c = a_c \cdot [Ca^{2+}]_{cyt}$, where a_a and a_c are constants. $[Ca^{2+}]_{cyt}$ seems to have no appreciable influence on endocytosis, k_d, or on the backward step, k_b. Figure 11B illustrates an example of experimental data and corresponding fit for one of five jointly fitted data sets. The example fit adequately describes the initial increase in C_m values in response to $[Ca^{2+}]_{cyt}$. The rate constants for the best data fits are listed in Table 1.

Using this model and the rate constants derived from joint fittings (Table 1), we simulated CARCs in response to an ideal $[Ca^{2+}]_{cyt}$ ramp. The curves illustrated in Figure 12 show the calculated time course of $[Ca^{2+}]_{cyt}$–stimulated increases in C_m values (1) for a common set of rate constants and (2) under the condition that pool A harbors different amounts of vesicles at the onset of the $[Ca^{2+}]_{cyt}$ increase. This variation in the size of pool A corresponds to the procedure of normalizing membrane capacitance data from different protoplasts to a common increase within the region of steep increase (Figure 5). The shapes of the simulated curves (Figure 12) and the experimental data (Figure 5) are very similar.

DISCUSSION

Our previous studies have shown that exocytosis in coleoptile cells is stimulated by micromolar concentrations of cytosolic Ca^{2+} (Thiel et al., 1994, 2000). Similar observations

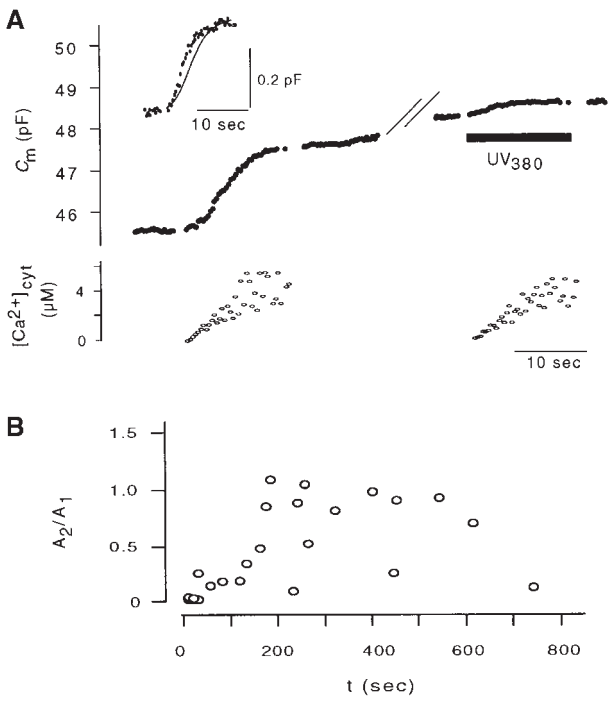

Figure 9. Recovery of CARC after Stimulation.

(A) In one protoplast, Ca^{2+} was increased (left) in ramplike fashion, resulting in CARC. After 155 sec, this procedure was repeated (right). Both procedures caused CARC with large (first stimulation) and low (second stimulation) amplitude. In the inset, the CARCs from the first stimulation (line) and from the second stimulation (dots) are scaled to the same ordinate.

(B) Ratio of amplitudes from second (A_2) and first (A_1) CARC as a function of the time between stimulations. Amplitudes were measured at isochronal times after $[Ca^{2+}]_{cyt}$–stimulated ΔC_m.

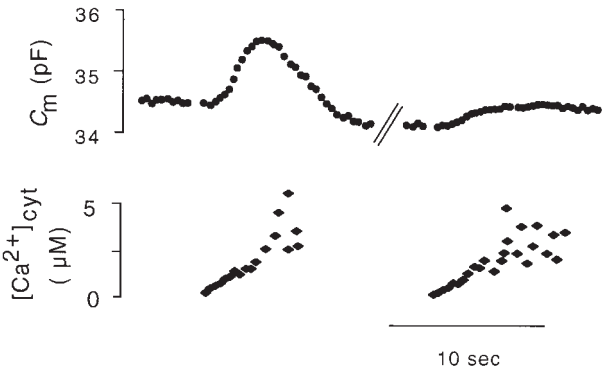

Figure 10. Recovery of CARC after a Preceding Endocytosis.

In one protoplast, $[Ca^{2+}]_{cyt}$ was increased in ramplike fashion (first stimulation, on the left), resulting initially in an increase and subsequently in a decrease in membrane capacitance. After 129 sec, $[Ca^{2+}]_{cyt}$ was increased a second time (second stimulation on the right). This second stimulation caused a CARC with an amplitude approximately one-third that of the first one.

have been reported for other plant cells (Zorec and Tester, 1992; Carroll et al., 1998, Homann and Tester, 1998), suggesting that $[Ca^{2+}]_{cyt}$ sensitivity may be a general feature of exocytosis in plant cells. The combined recording of $[Ca^{2+}]_{cyt}$ levels and membrane capacitance shows that C_m values exhibit a net increase when $[Ca^{2+}]_{cyt}$ concentrations are in the range of several hundred nanomoles per liter. Assuming that the resting level of $[Ca^{2+}]_{cyt}$ in coleoptiles is ~100 nM (Felle, 1988), it is evident that only moderate elevations of $[Ca^{2+}]_{cyt}$ are required to stimulate exocytosis. Variations in $[Ca^{2+}]_{cyt}$ of ~100 nM or more are indeed known to occur in coleoptile cells in response to the phytohormone indole-3-acetic acid (Felle, 1988). Accordingly, the sensitivity of the secretory system to $[Ca^{2+}]_{cyt}$ could be part of a stimulus–response coupling in these cells.

The rapid mobilization of Ca^{2+} from a caged precursor combined with recordings of membrane capacitance has enabled us to dissect the process of $[Ca^{2+}]_{cyt}$–stimulated secretion into distinct steps. From the sigmoidal change in C_m values after an increase in $[Ca^{2+}]_{cyt}$ and the kinetic modeling of this phenomenon, we can conclude that $[Ca^{2+}]_{cyt}$ stimulates at least two sequential steps in exocytosis: a stimulation of the final fusion step and enhanced refilling of a pool of vesicles ready for release from a pool of vesicles located upstream. Using these data, we are not able to detail the nature of the two discernible pools. However, the absence of a resolvable lag time for CARC elicited by the rapid increase of Ca^{2+} predicts that pool B must be located close to the plasma membrane when $[Ca^{2+}]_{cyt}$ –stimulated exocytosis begins. Only this proximity would allow such a rapid response of membrane capacitance to $[Ca^{2+}]_{cyt}$. Based on the maximal amplitude of CARCs (Figure 8), one can assume that this pool contains on average ~2.4% of the protoplast surface area in the form of vesicle membrane. Electron microscopy of grass coleoptiles has shown that these cells contain the equivalent of ~15% of their surface area in the form of secretory vesicles in the cytoplasm (Quaite et al., 1983). Against this background, we presume that pool B contains a subpopulation of the total number of morphologically detectable vesicles. The nature (and location) of pool A is less clear. It could, for example, reflect the vesicles traveling from the Golgi apparatus to the plasma membrane; it could also be a kinetic state of mature vesicles in the vicinity of the membrane and reflect vesicles that are, before fusion, either tethered or docked to the plasma membrane (e.g., Oheim et al., 1999; Pfeffer, 1999).

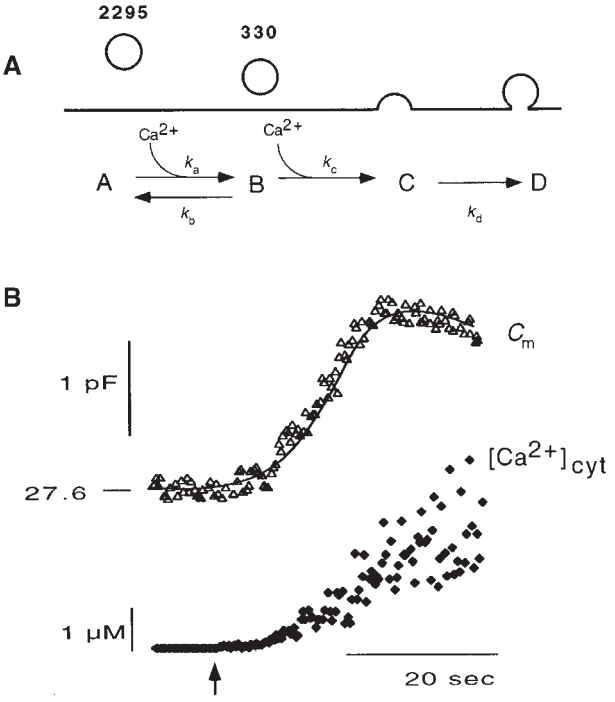

Figure 11. Kinetic Model for Secretion in Coleoptile Protoplasts and Fit of the Model to Experimental Data.

(A) Two-step model with two pools of vesicles (A and B) in series leading to exocytosis (pool C). Vesicles travel between pools A and B with the forward rate constants $k_a[Ca^{2+}]_{cyt}$ and $k_c[Ca^{2+}]_{cyt}$ and a backward rate constant k_b. Vesicles are reclaimed by endocytosis into pool D with a rate constant k_d. Numbers denote the number of vesicles in pools A and B that were obtained from fitting the data shown in **(B)**.

(B) Data from the simultaneous recording of C_m values and $[Ca^{2+}]_{cyt}$ in one coleoptile protoplast. At the times indicated by the arrow, Ca^{2+} was released from the DMN cage by UV_{380}. The solid line shows the fit to data with rate constants and pool sizes as given in **(A)**. The number on the membrane capacitance trace denotes the resting value in picofarads.

Both the experimental data and the modeling reflect the existence of endocytotic activity in these protoplasts. This view is consistent with observations of vesicle recycling observed in high-resolution capacitance measurements in protoplasts of the same type (Thiel et al., 1998). Furthermore, it is in line with quantitative analysis of electron micrographs from coleoptile cells, which showed that as many as 60% of the vesicles delivered to the plasma membrane are recycled (Phillips et al., 1988).

An interesting feature of the modeling was that all CARCs recorded in different protoplasts could be fitted with the same rate constants. This emphasizes that the reaction steps underlying the secretory pathway are very similar between cells. The variable shapes of the CARCs in different experiments can be solely ascribed to differences in the number of vesicles occupying pool A or pool B in the protoplasts examined. One explanation for this variability could be that different cells produce vesicles at different rates. Such a difference in vesicle synthesis has been shown in studies with coleoptile cells. Statistical analysis of electron micrographs from oats revealed that growing coleoptile cells averaged ~12% more vesicles per cubic micrometer of cytoplasm than did cells from nongrowing tissue (Quaite et al., 1983). Hence, the difference between individual cells could reflect the fact that the protoplasts originate from cells with different potentials for growth.

Overall, the general response of membrane capacitance to increases in $[Ca^{2+}]_{cyt}$ in coleoptile protoplasts is similar to that observed in neurons and can be described with a similar model, including multiple $[Ca^{2+}]_{cyt}$–sensitive steps (e.g., Heinemann et al., 1993, 1994). This similarity favors the suggestion that the molecular machinery of exocytosis is similar within eukaryotes; also, it is in line with the finding that plant cells also have many, if not all, of the proteins known to catalyze membrane fusion in animal cells (reviewed in Battey et al., 1999; Blatt et al., 1999). A great difference in the $[Ca^{2+}]_{cyt}$ sensitivity of exocytosis in coleoptile protoplasts versus that in animal cells is that in the latter cells, this process has a much steeper dependency on $[Ca^{2+}]_{cyt}$. For example, whereas $[Ca^{2+}]_{cyt}$ stimulates exocytosis in neuroendocrine cells in a third-order exponential manner (Heinemann et al., 1993), the sensitivity in the coleoptile protoplasts is only linear (Figure 11). In physiologic terms, this means that variations in $[Ca^{2+}]_{cyt}$ cause only a shallow increase in secretion in coleoptile cells, whereas the same variation has more dramatic effects on secretion in secretory animal cells.

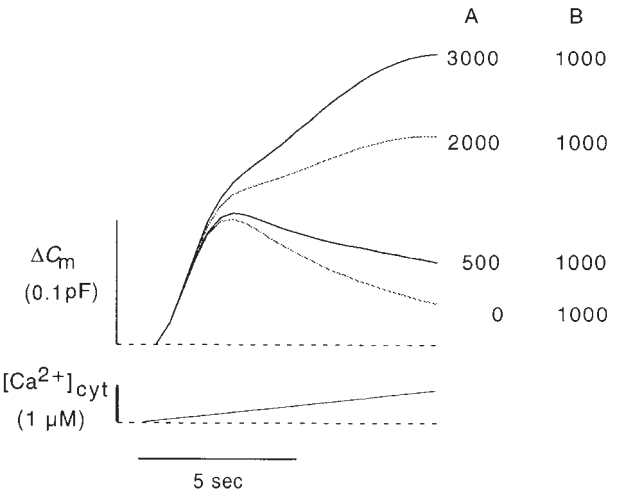

Figure 12. Simulation of CARC during Ramp Increases of $[Ca^{2+}]_{cyt}$.

Membrane capacitance curves (top) were calculated for linear $[Ca^{2+}]_{cyt}$ ramping (bottom) based on the model presented in Figure 11A and the rate constants from Table 1. Curves were calculated for different numbers of vesicles in pools A or B or both. The numbers of vesicles in the pools are given at right.

Table 1. Rate Constants for Model Presented in Figure 11A

Reaction Steps	Rate Constants (sec^{-1})[a]	Deviation[b]
k_a	$0.098[Ca^{2+}]_{cyt}$	±0.02
k_b	0.002	±0.015
k_c	$2.31[Ca^{2+}]_{cyt}$	±1.24
k_d	0.07	±0.017

[a] Rate constants obtained by jointly fitting five $C_m/[Ca^{2+}]_{cyt}$ data sets to the kinetic model given in Figure 11A.

[b] Mean deviation (±SD) between parameters obtained from fitting each experiment individually to those obtained by joint fit.

It is generally believed that plant cells undergo constitutive exocytosis exclusively, which means that the rate of secretion is determined by the rate of cargo, that is, vesicle production (Jones and Robinson, 1989). This view is consistent with our observation that the global rate of secretion is determined by the number of vesicles produced (that is, the number of vesicles that feed into serial pools). The role of Ca^{2+} in this scenario could be a modulating one. In this context, the rate of vesicle supply presumably must be coordinated with the rate of exocytosis. Assuming that the number of fusion sites on the plasma membrane is limited, it would be essential to increase the speed of the membrane fusion process to avoid a logjam of vesicles arriving at increased rates. Such a situation would occur during auxin-stimulated growth of coleoptiles when the rates of both vesicle and secretory cargo production as well as the presence of $[Ca^{2+}]_{cyt}$ all increase roughly within the same period of time (reviewed in Napier, 1995; Napier and Venis, 1995).

METHODS

Protoplasts were prepared as described previously (Thiel et al., 1994) and suspended in external solution containing 250 mM KCl, 10 mM

$CaCl_2$, 15 mM Mes-KOH, pH 6.1, and enough sorbitol to adjust the osmolarity to 600 mosmol kg^{-1}. The standard buffer solution contained 150 mM K-glutamate, 20 mM KCl, 5 mM $MgCl_2$, 2 mM Na_2ATP, 150 mM sorbitol, and 20 mM Hepes KOH, pH 7.2. Also EGTA and Ca-saturated EGTA were added to adjust the free calcium concentration.

Capacitance Measurements

Conventional whole-cell recordings (Hamill et al., 1981) were performed with wax-coated pipettes of 2 to 3 MΩ resistivity. An EPC-9 patch–lamp amplifier (HEKA Electronics, Lambrecht, Germany) was used with PULSE software (HEKA). Cell capacitance was obtained with the software lock-in extension of the PULSE program based on the Lindau-Neher technique (Gillis, 1995; 1-kHz sinusoid stimulus with 20-mV peak-to-peak amplitude). Cells were held at −50 mV, a condition in which current–voltage relations were almost linear in the whole-cell configuration (Thiel and Weise, 1999). Measurements were considered for analysis only in cases in which the access conductance was >100 nS (i.e., > $M\Omega^{-1}$).

Photolysis of Caged Ca^{2+} and Ca^{2+} Measurements

For increasing the concentrations of free Ca^{2+} in the cytoplasm ($[Ca^{2+}]_{cyt}$), protoplasts were perfused from the patch pipette with a solution containing 280 mM potassium glutamate, 20 mM KCl, 20 mM Hepes-KOH, pH 7.5, 10.9 mM 1-(2-nitro-4,5-dimethoxyphenyl)-1,2-diaminoethane-*N*,*N*,*N′N′*-tetraacetic acid dimethoxynitrophenamine sodium (DMN), 5 mM $CaCl_2$, and 0.4 mM fura-2. Before photorelease, this medium buffered $[Ca^{2+}]_{cyt}$ to ~4 nM (Xu et al., 1997). Because the fluorescence excitation wavelength for $[Ca^{2+}]_{cyt}$ measurements with fura-2 also covers the UV range that photolyses DMN, we used fluorescence excitation light at 380 nm to measure $[Ca^{2+}]_{cyt}$ and photorelease Ca^{2+} concentrations from the caged precursor simultaneously. An aperture in the UV light path ensured that only the Ca^{2+} within the protoplast was liberated. Different rates of Ca^{2+} release were achieved by placing neutral density filters into the pathway of the excitation light.

During these single-wavelength measurements, in which the initial fluorescence, F_0, is approximately equal to the maximal fluorescence, F_{max}, the change in fluorescent signal over time, F_t, was used to estimate $[Ca^{2+}]_{cyt}$, according to Xu et al. (1997), as follows:

$$[Ca^{2+}]_{cyt} = k_d \frac{1 - F_{(t)}/F_{(0)}}{F_{(t)}/F_{(0)} - F_{(min)}/F_{(max)}} \quad (1)$$

A k_d value of 205 nM was obtained by in vivo calibration of fura-2, according to Neher (1989). The minimum fluorescence, F_{min}, was measured after constant illumination with UV light at the end of the experiment. F_{max} was obtained from the initial F_{380} value recorded at the onset of illumination. A line was fitted through the F_{380} data obtained after complete mobilization of Ca^{2+} and was used to estimate the contribution of photobleaching (Xu et al., 1997). The latter value was then considered in the calculation of $[Ca^{2+}]_{cyt}$.

In control experiments, we monitored the time over which the cytoplasm was perfused from the pipette under our conditions. For these experiments, we omitted DMN and $CaCl_2$ from the pipette solution and measured the increase in fura-2 concentration in the cytoplasm after breaking into the whole-cell configuration. This was achieved by recording the fluorescence at the isosbestic wavelength (360 nm) after breaking into the whole-cell configuration. We found that on average, it took 115 ± 31 sec ($n = 7$) before the fluorescence reached 90% of the maximum.

DMN was purchased from Calbiochem (Bad Sod, Germany), and fura-2 was from Molecular Probes (Eugene, OR). All other chemicals were from Sigma-Aldrich.

Modeling

The first-order differential equations derived from the model (Figure 11A) and the equations for the rate constants are listed below:

$$dA/dt = k_o E + k_b B - k_a A, \text{ with } E = A10^3 \quad (2)$$

$$dB/dt = k_a A - (k_b + k_c) B \quad (3)$$

$$dC/dt = k_c B - k_d C \quad (4)$$

$$k_o = a_o,\ k_a = a_a[Ca^{2+}]_{cyt},\ k_c = a_c[Ca^{2+}]_{cyt},\ k_b = a_b, \text{ and } k_d = a_d \quad (5)$$

where a_o, a_a, a_b, a_c, and a_d are constants; E represents the membrane reservoir available downstream of the site of vesicle production; A and B are vesicle pools in the secretory pathway; and C is the amount of membrane inserted into the plasma membrane as a result of exocytosis. The various k_x values are the rate constants for vesicle movement between the different pools.

Fits were obtained by the Simplex algorithm, which is a fitting algorithm that uses a geometric construct rather than differentials (Nedler and Mead, 1965; Cacci and Cacheris, 1984). This method allows very precise calculation and easy implementation of a joint fitting routine. Because refilling experiments (Figure 9) showed rate constant k_o to be negligible compared with the other four rate constants, Equation 2 was simplified to the following form:

$$dA/dt = k_c B - k_a A \quad (6)$$

Fits were accepted when the calculated curves matched the measured data trace within the range of the noise level (~35 fF).

ACKNOWLEDGMENTS

We are grateful to Dietrich Gradmann (Göttingen, Albrecht v. Haller Institute, Biophysics) for many helpful suggestions. This work was supported by Deutsche Forschungs–gemeinschaft Grant No. SFB523.

Received January 3, 2000; accepted May 1, 2000.

ACKNOWLEDGMENTS

Battey, N.H., James, N.C., Greenland, A.J., and Brownlee, C. (1999). Exocytosis and endocytosis. Plant Cell **11,** 643–659.

Blatt, M.R., Layman, B., and Geelen, D. (1999). Molecular events of vesicle trafficking and control by SNARE proteins in plants. New Phytol. **144,** 389–418.

Cacci, M.S., and Cacheris, W.P. (1984). Fitting curves to data—The simplex algorithm is the answer. BYTE **5,** 340–362.

Carroll, A.D., Moyen, C., Van Kesteren, P., Tooke, F., Battey, N., and Brownlee, C. (1998). Ca^{2+}, annexins, and GTP modulate exocytosis from maize root cap protoplasts. Plant Cell **10,** 1267–1276.

Felle, H. (1988). Auxin causes oscillations of cytosolic free calcium and pH in *Zea mays* coleoptiles. Planta **174,** 495–499.

Gillis, K.D. (1995). Techniques for membrane capacitance measurements. In Single Channel Recording, 2nd ed, B. Sakmann and E. Neher, eds (New York: Plenum Press), pp. 155–198.

Hamill, O.P., Marty, A., Neher, E., Sakmann, B., and Sigworth, F.J. (1981). Improved patch-clamp technique for high resolution current recordings from cells and cell-free membrane patches. Pflügers Arch. Eur. J. Physiol. **391,** 85–100

Heinemann, C., von Rüden, L., Chow, R.H., and Neher, E. (1993). A two-step model of secretion control in neuroendocrine cells. Pflügers Arch. Eur. J. Physiol. **424,** 105–112.

Heinemann, C., Chow, R.H., Neher, E., and Zucker, R.S. (1994). Kinetics of the secretory response in bovine chromaffin cells following flash photolysis of caged Ca^{2+}. Biophys. J. **67,** 2546–2557.

Homann, U., and Tester, M. (1997). Ca^{2+}-independent and Ca^{2+}/GTP-binding protein–controlled exocytosis in a plant cell. Proc. Natl. Acad. Sci. USA **94,** 6565–6570.

Homann, U., and Tester, M. (1998). Patch-clamp measurements of capacitance to study exocytosis and endocytosis. Trends Plant Sci. **3,** 110–114.

Jones, R.L., and Robinson, D.G. (1989). Tansley Review No. 17: Protein secretion in plants. New Phytol. **111,** 567–597.

Kasai, H. (1999). Comparative biology of Ca^{2+}-dependent exocytosis: Implications of kinetic diversity for secretory function. Trends Neurosci. **22,** 88–93.

Napier, R.M. (1995). Towards an understanding of ABP1. J. Exp. Bot. **46,** 1787–1795.

Napier, R.M., and Venis, M.A. (1995). Auxin action and auxin-binding proteins. New Phytol. **129,** 167–201.

Nedler, J.A., and Mead, R. (1965). A simplex method for function minimization. Comput. J. **7,** 308.

Neher, E. (1989) Combined fura-2 and patch clamp measurements in rat peritoneal mast cells. In Neuromuscular Junction, L.C. Sellin, R. Libelius, and S. Thesleff, eds (Amsterdam: Elsevier Science), pp. 65–76.

Neher, E., and Marty, A. (1982). Discrete changes of cell membrane capacitance observed under conditions of enhanced secretion in bovine adrenal chromaffin cells. Proc. Natl. Acad. Sci USA **79,** 6712–6716.

Oheim, M., Loerke, D., Stühmer, W., and Chow, R.H. (1999). Multiple stimulation-dependent processes regulate the size of the releasable pool of vesicles. Eur. Biophys. J. **28,** 91–101.

Pfeffer, S.R. (1999). Transport-vesicle targeting: Tethers before SNAREs. Nat. Cell Biol. **1,** 17–22.

Phillips, G.D., Preshaw, C., and Steer, M.W. (1988). Dictyosome vesicle production and plasma membrane turnover in auxin-stimulated outer epidermal cells of coleoptile segments from *Avena sativa* (L.). Protoplasma **145,** 59–65.

Quaite, E., Parker, R.E., and Steer, M.W. (1983). Plant cell extension: Structural implications for the origin of the plasma membrane. Plant Cell Environ. **6,** 429–432.

Thiel, G., and Weise, R. (1999). Auxin augments conductance of K^+ inward rectifier in maize coleoptile protoplasts. Planta **208,** 38–45.

Thiel, G., Rupnik, M., and Zorec, R. (1994). Raising the cytosolic Ca^{2+} concentration increases the membrane capacitance of maize coleoptile protoplasts: Evidence for Ca^{2+}-stimulated exocytosis. Planta **195,** 305–308.

Thiel, G., Kreft, M., and Zorec, R. (1998). Unitary exocytotic and endocytotic events in *Zea mays* coleoptile protoplasts. Plant J. **13,** 101–104.

Thiel, G., Sutter, J.-U., and Homann, U. (2000). Ca^{2+}-sensitive and Ca^{2+}-insensitive exocytosis in maize coleoptile protoplasts. Pflügers Arch. Eur. J. Physiol. **439** (suppl.), 152–153.

Xu, T., Naraghi, M., Kang, H., and Neher, E. (1997). Kinetic studies of Ca^{2+} binding and Ca^{2+} clearance in the cytosol of adrenal chromaffin cell. Biophys. J. **73,** 532–545.

Zorec, R., and Tester, M. (1992). Cytoplasmic Ca^{2+} stimulates exocytosis in a plant secretory cell. Biophys. J. **63,** 864–867.